Drying the Wetland: Water Scarcity in the Brazilian Pantanal*

Vinícius Hector† Rafael Araujo‡ Francisco Costa§

February 2026

Abstract

This paper examines the impact of upstream deforestation on water coverage and burned area in wetlands. Using a panel dataset of satellite-derived land cover for multiple hydrographic basins, we analyze this relationship in the Brazilian Pantanal from 1985 to 2023. We find that a 1% increase in upstream deforestation reduces water coverage by 0.51% and increases burned area by 0.55% per year. The effect of upstream deforestation on downstream burned area generates an emissions multiplier, as carbon released through deforestation is compounded by emissions from downstream burned area. On average, for each ton of carbon emitted due to deforestation, an additional 0.14 tons are released through downstream fire.

JEL: *Q23, Q56, Q15, Q25*
Keywords: *Climate, Deforestation, Water, Land Use, Wetland*

*We would like to thank Ariaster Chimeli, Sophie Mathes, Molly Lipscomb, and referees for helpful comments. We gratefully thank the financial support from CAPES/Brasil.
†FGV EPGE. E-mail: vinicius.hector@outlook.com.br
‡FGV EESP Sao Paulo School of Economics. E-mail: rafael.araujo@fgv.br
§FGV EPGE. E-mail: francisco.costa@fgv.br

1 Introduction

Water connects distant regions through both surface and atmospheric flows, creating interdependencies that are difficult to account for in local and global governance. This complexity exposes water systems to suboptimal resource use across space, especially when externalities can lead to a tragedy of the commons. Recognizing the hydrological cycle as a shared system is a crucial step toward improving water governance and ensuring more efficient allocation of resources (Global Commission on the Economics of Water, 2024). Recent research has examined these issues in the context of irrigation and water markets (Rafey, 2023), pollution (Lipscomb and Mobarak, 2017), and floods (Taylor and Druckenmiller, 2022).

This paper investigates the impact of deforestation on downstream water coverage and burned area in the world's largest wetland, the Pantanal. The Pantanal, located in the heart of South America, is a large flooded plain spanning over 195,000 km^2 across Brazil, Bolivia, and Paraguay — an area comparable to Great Britain or ten times the size of the Everglades in Florida. The biome hosts a rich flora and fauna, with over 4,700 species of animals and plants. It is also home to approximately three million people, with cattle ranching as its leading economic activity (WWF, 2018). However, the region has been experiencing sustained drying. MapBiomas Brasil (2024) show that water coverage in the biome declined from 15.4% of the biome's area in the late 1980s to only 3.6% in 2023, a total loss of 18,100 km^2 of water. The significant decrease in water coverage can make the entire biome more prone to the spread of fires during droughts.

There is an ongoing debate about the primary drivers of this drying trend. While there is broad agreement that the Pantanal has become systematically drier in recent decades (Rosa et al., 2025; Libonati et al., 2020), there is no consensus on its underlying causes. Some researchers attribute the decline in water coverage primarily to reduced rainfall in the Cerrado highlands, where the headwaters of the Pantanal's rivers originate (Marengo et al., 2021; Lázaro et al., 2020; Bergier et al., 2018). Others argue that deforestation is the main driver, as it reduces soil infiltration and impairs river recharge, thereby lowering water availability during the dry season (Santos et al., 2024; Ivory et al., 2019; Leal Filho et al., 2021). This paper contributes to the debate by empirically quantifying the importance of these two mechanisms in explaining the observed decline in water coverage and the Pantanal's diminished capacity to contain fire.

To address this question, we construct a new panel dataset spanning 1985 to 2023, combining annual data on water coverage, burned area, rainfall, and upstream deforesta-

tion across hydrographic basins. To exploit the long panel structure, we employ a first-difference estimator to recover the causal impact of upstream deforestation and rainfall on downstream water coverage and burned area.

Our main finding shows that deforestation — primarily driven by pasture expansion — has significantly reduced water coverage and increased burned area downstream. Specifically, a 1% increase in upstream deforestation leads to a 0.51% decline in downstream water coverage and a 0.55% increase in burned area. Additionally, with the within-basin year-to-year variation we use, we find no evidence that upstream rainfall affects downstream water coverage, indicating that observed rainfall changes have not been sufficient to affect water coverage in the Pantanal. The downstream impact of burned area caused by deforestation creates a multiplier effect on emissions associated with deforestation. We estimate that deforestation alone resulted in approximately 1.029 billion metric tons of CO_2 emissions between 1985 and 2023. Based on our elasticity estimate for burned area, the downstream spillover linked to increased fire occurrence accounts for an estimated 151 million metric tons of CO_2. This spillover effect represents nearly 14% [0.151/1.029] of the total emission attributed directly to deforestation.

To strengthen the causal interpretation of our results, we conduct two placebo tests. First, as water does not travel upriver, we invert the construction of our data to estimate the impact of *downstream* deforestation on water coverage. We find a null result in this specification. Second, we find no significant effect of future deforestation on water coverage and burned area. Both placebos are supporting evidence that our main results are not driven by omitted variables or spurious spatial correlations.

Our paper is connected with different strands of the literature. As discussed earlier, recognizing the hydrological cycle is crucial when studying local and global governance of water resources. For example, Lipscomb and Mobarak (2017); Chen et al. (2018); Yu et al. (2018) study reallocation of pollution as a result of different governance of rivers, and Ebenstein (2012); Dias et al. (2023); Skidmore et al. (2023) show how contaminants travel through waterways, generating health impacts far from their source. Closely related to our paper, Karwowski (2024) shows the impact of wetland conservation on agricultural productivity. We contribute to this literature by studying a different mechanism by which accounting for the hydrological system becomes important, that of connecting deforestation and the decrease in water coverage and the increase in burned area.

The connection between land use change and water dynamics has been explored in the context of wetland suppression and flooding in the United States (Brody et al., 2015; Sun

and Carson, 2020; Taylor and Druckenmiller, 2022; Aronoff and Rafey, 2023). These studies emphasize the role of wetlands as natural buffers that absorb excess water and reduce flood risk in urban developed areas. In contrast, our paper examines how upstream deforestation affects the ability of an entire biome to regulate its water cycle, undermining its stability and resilience to dry-season fires. While much of the literature on flooding focuses on valuing wetlands through their flood prevention services, we take a different approach by quantifying a multiplier effect in carbon emissions—one that emerges only when accounting for spillovers from deforestation through the river system.

Although some areas of the Pantanal biome are designated as protected by the Brazilian government—to safeguard its ecological stability, biodiversity, and carbon stock—these protections are limited by the fact that the biome is surrounded by upstream non-protected areas. This regulatory design overlooks the hydrological interdependencies between basins, allowing external land-use changes to undermine internal conservation efforts. Existing discussions on the optimal allocation of water resources have largely focused on market-based mechanisms (Rafey, 2023; Hagerty, 2023). While we do not model optimal prices or allocations, our findings provide an important contribution to this debate by demonstrating that upstream deforestation generates downstream spillovers that must be considered in any governance scheme. Given the complexity of the Pantanal's hydrological network—which includes thousands of interconnected sub-basins—market-based allocations may be suboptimal when information is costly to acquire. In such cases, expanding protected areas could offer a more efficient policy response, linking our analysis to the broader debate on regulation through prices versus quantities (Weitzman, 1974).

Our paper also contributes to the large literature on deforestation (Burgess et al., 2023; Assunção et al., 2013, 2020; Souza-Rodrigues, 2019; Domínguez-Iino, 2026; Sant'Anna, 2021; Araujo et al., 2026), which has largely overlooked the hydrological consequences of deforestation transmitted through river systems. Ignoring these effects may lead to underestimating the benefits of policies aimed at reducing deforestation or overestimating the gains from agricultural land expansion.

Finally, as discussed before, a substantial body of literature in the natural sciences has examined the recent changes in the Pantanal. Yet, there remains no consensus on the primary cause—whether it stems from reduced rainfall in the surrounding highlands (Marengo et al., 2021; Lázaro et al., 2020; Bergier et al., 2018) or from deforestation (Santos et al., 2024; Ivory et al., 2019). Our contribution is to empirically test these hypotheses within a framework that enables a clear discussion on identification and statistical inference.

The remainder of the paper is structured as follows: Section 2 discusses the Pantanal's hydrology and how deforestation can lead to water scarcity. Section 3 describes the data sources and the panel construction. Section 4 outlines the empirical methodology. Section 5 presents the results. Section 6 concludes.

2 Background

The Pantanal is the world's largest wetland. Situated in central South America, it is a vast floodplain covering roughly 195,000 km^2 across Brazil, Bolivia, and Paraguay, an area as large as Great Britain. The region has a remarkable biodiversity, hosting more than 4,700 species of flora and fauna. It is also inhabited by around three million people, with cattle ranching serving as the primary economic activity (WWF, 2018).

The Pantanal exists due to the unique mix between its topography and hydrological cycle. Its relief resembles a plate, forming a flat plain surrounded by highlands, as shown in (see Figure A1 in the Appendix). Rainfall and groundwater recharge feed rivers originating in these highlands (Bergier, 2013; Paz et al., 2011; WWF, 2018). This water follows three possible paths: it flows downstream to flood the plain before draining into the Paraguay River, it infiltrates the soil for storage and later release, or it evaporates.[1]

Natural vegetation is crucial for maintaining the balance of the biome. During the wet season (October to March), heavy rainfall feeds rivers and gravity carries water downstream, flooding up to two-thirds of the plain (WWF, 2018). As the Pantanal is a low-altitude plain with only one natural drain - the Paraguay River - most of the seasonal rainwater accumulates in lagoons. In this context, vegetation around the headwaters acts like a sponge, absorbing and retaining water to later release (Peña-Arancibia et al., 2019; Rohde et al., 2021). During the dry season (April to September), there is almost no precipitation, and the lagoons mostly dry naturally. Then, the stored groundwater is gradually released, sustaining the naturally reduced river flow. This last mechanism preserves the biome's lagoons at reduced levels and ensures the stability of the ecosystem until the next wet season.

However, water coverage in the Pantanal has declined dramatically since the 1980s (Figure 1). Between 1985 and 2023, the biome experienced an 83% reduction in water-covered areas during the dry season. While water covered 21% of the Pantanal in 1985, this figure had dropped to just 3.6% by 2023. At the same time, recent years have seen some of

[1] Part of the infiltrated water feeds the vegetation, which is known as 'Green Water' (Global Commission on the Economics of Water, 2024).

Figure 1: Upper Paraguay River Basin Water and Deforestation Evolution (1985 - 2023)

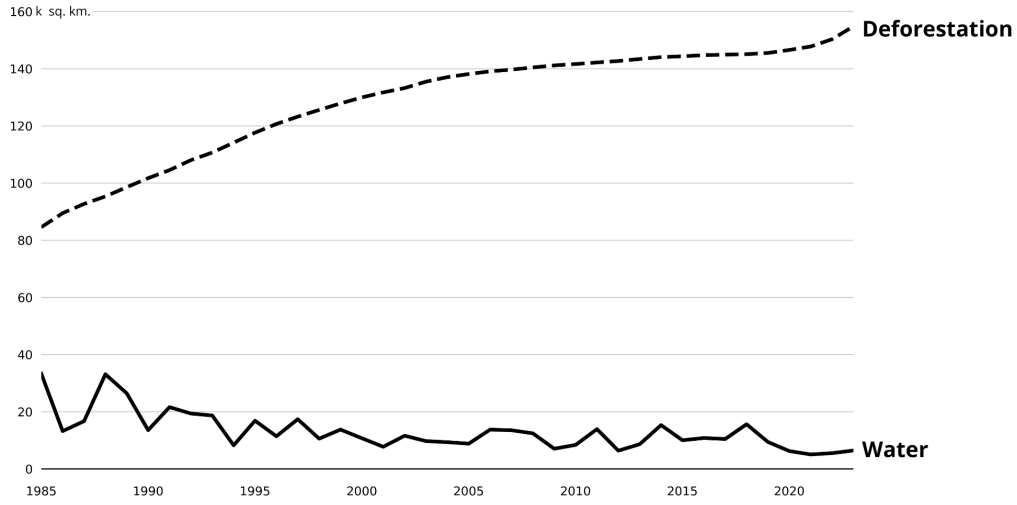

Notes: The chart shows annual water and deforestation cover in km^2 for the Upper Paraguay River Basin. This region includes both the Pantanal plain and the surrounding Cerrado highlands.

the most extreme fire seasons on record, even though the average yearly burned area has slightly decreased. In 2020, for example, the Pantanal faced its second most intense fire season, with wildfires that consumed 16% of the biome, four times the average burned area between 1985 and 2023 (MapBiomas Brasil, 2024). Figure 2 illustrates the evolution and spatial distribution of land cover changes across the region in that period.

3 Data

To study the impact of deforestation on downstream water coverage and burned area, we gather data on hydrographic basins, land cover, and rainfall. Below, we describe each of these data sets.

3.1 Hydrographic Basins

Hydrographic basins, or simply basins, are our primary units of observation. A basin is the land area where all water converges to a single point. Topography determines the boundaries of a basin and it can be subdivided into up to nine smaller sub-basins following the Pfafstetter Coding Method (also known as Ottocodification).[2] This method en-

[2] ANA (2006) outlines the technical details of the Pfafstetter Coding Method. The core concept involves identifying a basin and its main river, as well as locating the four main tributaries and their corresponding

Figure 2: Four Decades of Land Cover Change

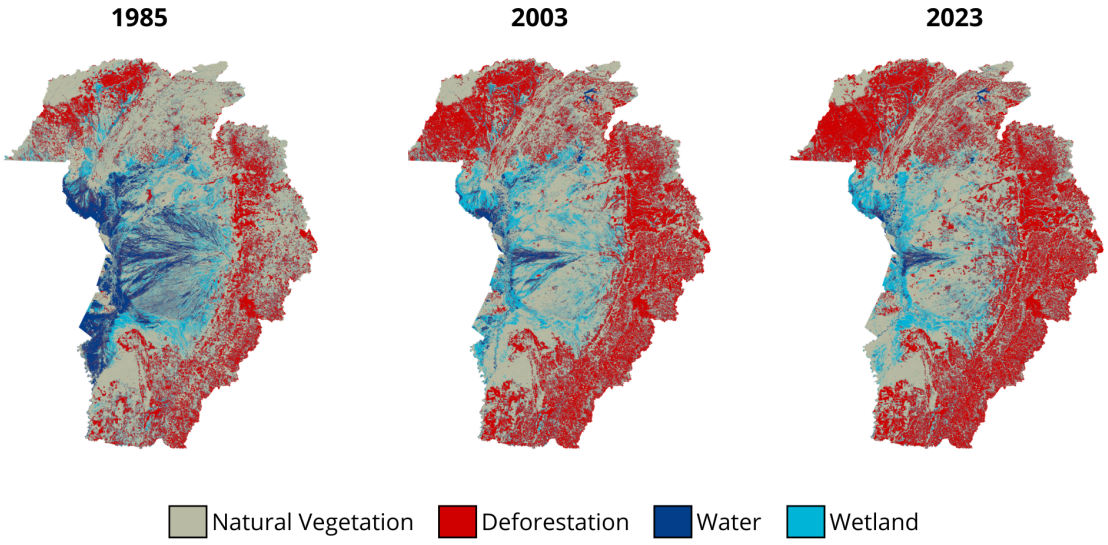

Notes: These maps show the evolution of land cover in the Brazilian Pantanal, over the last four decades. Natural vegetation mainly consists of forests, savannas, and grassland. Deforestation consists of pasture, agriculture, mining, and cities. Notice the stark decrease in water coverage throughout the years.
Source: MapBiomas Brasil (2024)

ables the systematic organization of a region's hydrography and identifies the upstream and downstream basins relative to a given basin (ANA, 2006).

We use data from ANA (2020) to outline Pantanal's hydrographic basins. There are seven basin levels. In this paper, we use level 6 basins, the second most granular level, and subset to all basins within the Brazilian part of the Upper Paraguay Hydrographic Basin.[3] This results in 1,873 level 6 basins, whose water ultimately flows to the Paraguay River, which discharges in the Paraná River, eventually discharging into the Atlantic Ocean.

The Pfafstetter Coding System allows us to define the set of downstream basins given a generic basin. Using a backward-looking algorithm, we then find all upstream basins. Running this algorithm on all basins in the panel, we find the upstream and downstream areas for each level 6 watershed. Figure A2 in the Appendix shows an example of the Ottocodification.

catchment areas. These tributaries are assigned even numbers from 2 to 8, ordered from downstream to upstream. The remaining areas of the basin are subsequently divided and numbered using the same algorithm. This iterative approach delineates N+1 level sub-basins within an original level N basin.

[3]We consider all level 6 basins with at least 90% of its area in Brazil within the level 2 basin code 89 - the Upper Paraguay Hydrographic Basin

3.2 Land Cover and Fire

We use MapBiomas Brasil (2024) to get land use and land cover (LULC) data within each basin and their upstream and downstream areas. MapBiomas cleans Landsat satellite imagery to generate high-resolution rasters that classify LULC at a 30m × 30m resolution across Brazil from 1985 to 2023. We subset and aggregate this dataset to align with the spatial units of interest.

We define deforested areas as anthropogenic land use, which includes pixels classified as pasture, agriculture, mining, and urban areas. Natural land use includes forests, grasslands, savannas, water, and wetlands.[4] Water refers to permanent rivers and lakes, while wetlands are areas (usually grasses) subject to permanent or temporary flooding. The key difference is that wetlands dry seasonally, whereas water bodies remain permanent. This distinction is crucial for our analysis as many of the drying water bodies are transitioning into wetland areas.

MapBiomas methodology for the Pantanal accounts for the biome's hydrological cycle by relying on satellite imagery only from the dry season (MapBiomas Brasil, 2025a). The Cerrado module also captures images between May 1st and August 30th of each year, to ensure consistency. As a direct consequence, this study examines the effects of upstream deforestation on downstream water availability in the Pantanal during the dry season, when water scarcity and fire occurrences are most frequent. Due to the dataset's temporal constraints, we cannot analyze how these processes unfold during the wet season. Nonetheless, the most extensive wildfires and significant ecological imbalances occur during the dry season, which the dataset captures properly.

We also obtain yearly burned area data from MapBiomas Brasil (2024), which relies on satellite imagery from Giglio et al. (2015); Long et al. (2019); Instituto Nacional de Pesquisas Espaciais (INPE) (2023). They use a similar algorithm to detect if a 30m × 30m pixel was affected by fire in a given year. Since wildfires occur during the dry season (april to september), this dataset primarily captures fire occurrences in the same period as the LULC module for both biomes. To quantify burned areas at the basin-year level, we apply a methodology similar to that used for LULC data aggregation and end up with the yearly burned area (in km^2) for each basin.

We combine the basins' data described in section 3.1 with both data on land cover and fire

[4]Specifically, anthropogenic land use corresponds to MapBiomas classifications under code 14 (agriculture and pasture) and code 22 (non-vegetated area). The latter includes codes 24 (urban area), 25 (other non-vegetated regions), and 30 (mining). The remaining codes are considered natural land cover. See (MapBiomas Brasil, 2025b) for a complete description of LULC categories.

to build a panel where, for each year-basin, we measure its water coverage, burned area, and upstream deforestation. Figure A3 in the Appendix presents an example of LULC classification of a basin and its upstream area. We run this algorithm for all 1,873 basins in all 39 years, yielding a panel of 73,047 observations.

3.3 Rainfall

We also investigate the impact of upstream rainfall on downstream water coverage and burned area. We get yearly rainfall estimates from the Climate Hazards Group InfraRed Precipitation with Station (CHIRPS) dataset to do so. Climate Hazards Center (2023) integrates satellite precipitation estimates with ground-based observations to generate high-resolution rainfall data (in mm per year). Its rasters cover 5 km × 5 km grid cells for latitudes between 50°S and 50°N since 1981. We apply a similar algorithm to calculate upstream rainfall for each basin-year.

Table 1: Summary Statistics

	Mean	Std. Dev.	P25	Median	P75
Basin Area (km^2)	144.97	331.93	9.49	37.84	123.71
Water in Basin (km^2)	11.55	34.49	0.19	1.60	8.19
Fire in Basin (km^2)	7.35	36.50	0.00	0.02	1.65
Upstream Deforestation (km^2)	15,270.66	27,753.80	4.76	637.72	19,461.48
Upstream Rainfall (mm)	1,258.63	239.93	1,099.89	1,262.23	1,432.16

Notes: This table reports summary statistics for the main variables in the panel. All variables are measured at the basin-year level. Basin Area, Water in Basin, Fire in Basin, and Upstream Deforestation are measured in km^2. Upstream Rainfall is measured in millimeters of annual precipitation. We restrict the summary statistics to the 1,052 basins located within the Pantanal plain over a 39-year period, resulting in $1{,}052 \times 39 = 41{,}028$ observations in the panel. For Upstream Deforestation and Upstream Rainfall, we report statistics only for open basins, as closed basins have zero values for both variables. As a result, the number of observations for these two variables is nearly half that of the others ($535 \times 39 = 20{,}865$).

3.4 Summary Statistics

Our panel considers all 1,873 level-6 basins located within the Upper Paraguay hydrographic region inside Brazilian territory. Following the availability of MapBiomas data, the panel spans the full 39-year period from 1985 to 2023.

The panel covers both the lowland basins of the Pantanal plain and those located in the surrounding Cerrado highlands (see Figure A1). Of these, 1,052 basins – or 56% of the total

– are located within the Pantanal plain. These are the basins for which we observe water and fire dynamics, and they serve as the basis for our main estimations. However, data from all 1,873 basins are used to construct upstream measures. This distinction is central to our analysis: we investigate whether the expansion of deforestation in the whole hydrographic region - the Cerrado highlands and the Pantanal plain - affects water balance and fire occurrence downstream in the Pantanal plain. Table 1 shows descriptive statistics of all variables.

4 Empirical Methods

4.1 Specification

Our goal is to estimate the causal effect of upstream deforestation – mainly to pasture and agriculture – on downstream water coverage and burned area. To achieve this, we construct a panel dataset and employ a first-difference specification.

In our main specification, we analyze how upstream deforestation influences downstream water coverage and burned area through the following equation:

$$\Delta \operatorname{arcsin}(y_{it}) = \beta_t + \beta \Delta \operatorname{arcsin}(\text{UpDeforestation}_{it}) + \gamma \Delta \operatorname{arcsin}(\text{UpRainfall}_{it}) + \Delta \epsilon_{it} \quad (1)$$

where y_{it} denotes either water coverage or burned area, and $UpDeforestation_{it}$ denotes upstream deforested area in basin i, year t. We measure areas in km^2 for water coverage and burned area, and then apply the inverse hyperbolic sine transformation. This allows us to deal with the zeros in our data at the same time the estimated coefficients represent elasticities, indicating the average percentage impact of a 1% increase in the associated regressor.[5] The term $\Delta \operatorname{arcsin}(y_{it})$ represents the first-difference of the inverse hyperbolic sine transformation, as does $\Delta \operatorname{arcsin}(UpDeforestation_{it})$. The term β_t is a dummy variable that equals one if the observation is in year t and zero otherwise, a year fixed effect. Basin fixed-effect is eliminated by the first-difference. In some specifications, we control by changes in upstream rainfall, $\Delta \operatorname{arcsin}(\text{UpRainfall}_{it})$. Standard errors are clustered at level 5 basins, as suggested by Dias et al. (2023).[6] This allows us to account for spatial correlation among the basins in the same region and work as a spatial cluster.

[5] $\operatorname{arsinh}(x) = \ln\left(x + \sqrt{x^2+1}\right)$ is a monotonic transformation analogous to $\log(x)$, but it is defined at zero. See Bellemare and Wichman (2020); Aïhounton and Henningsen (2019) for a detailed discussion of inverse hyperbolic sine transformation.

[6] Recall from Section 3 that we use level 6 basins as the basic unit of observation. Each level 5 basin contains up to 9 level 6 ones.

We employ the first-difference estimator with year dummies instead of a two-way fixed effects specification due to the long panel structure of our data, as discussed in Millimet and Bellemare (2025). As the panel length increases, the assumption that unit-specific unobserved heterogeneity remains time-invariant becomes less realistic. Unlike the two-way fixed effects, which relies on this assumption and removes such heterogeneity by demeaning the variables using data for all years, the first-difference estimator progressively eliminates slow time-variant heterogeneity through sequential subtraction year after year. This approach offers a more realistic treatment of slow time-variant unit characteristics, thereby mitigating potential biases arising from dynamic, unobserved confounders. Ignoring that it is unrealistic to assume time-invariant basin characteristics in a time span of four decades would likely lead to a violation of the strict exogeneity assumption, which is not required in a first-difference estimator that only requires sequential exogeneity (see e.g., Anderson and Hsiao, 1981; Arellano and Bond, 1991). This is particularly important in our setting because the water coverage in Pantanal may also be determined by climate cycles (Bergier and Assine, 2022).[7]

The identification strategy relies on the assumption that changes in upstream deforestation are uncorrelated with changes in other factors that could influence downstream water coverage and burned area. Thus, the main threat to our identification is omitted variable bias. To strengthen the causal interpretation of our results, we implement a placebo test using downstream deforestation as a regressor.

A statistically significant relationship between upstream deforestation and downstream water coverage provides evidence that deforestation change affects hydrological dynamics, likely through mechanisms such as reduced infiltration and increased sedimentation that disrupt river flows and spring recharge—contributing to the Pantanal's drying and increased fire risk (Santos et al., 2024). In contrast, a null relationship would suggest that broader forces, such as climate change, may be the dominant drivers of the observed hydrological imbalances.

As an additional placebo test, we include a lead of deforestation in our first-difference specification. Given the differentiated structure of the specification, this amounts to testing whether future changes in forest cover explain current changes in downstream water

[7] A simple way of illustrating it is assuming a data generating process as $y_{it} = \alpha + \beta x_{it} + \alpha_{it} f(t) + \epsilon_{it}$. A first-difference would yield: $\Delta y_{it} = \beta \Delta x_{it} + \alpha_{it} \Delta f(t) + \tilde{\epsilon}_{it}$, and $\alpha_{it} \Delta f(t)$ would become an omitted variable. While a demeaning difference would yield: $y_{it} - \bar{y}_{it} = \beta(x_{it} - \bar{x}_{it}) + \alpha_{it}(f(t) - f(\bar{t})) + \tilde{\epsilon}_{it}$, and $\alpha_{it}(f(t) - f(\bar{t}))$ would become an omitted variable. Analyzing the omitted variables, if $f(t)$ changes slowly, then $\Delta f(t) \approx 0$ while $f(t) - f(\bar{t})$ can increase with the length of the panel. That is why we use yearly differences, which is the most granular temporal variation we have, so that $f(t + \Delta t) - f(t)$ is as small as possible.

cover and fire incidence. Under our identification assumptions, such predictive effects should not arise.

5 Results

Table 2 presents the coefficients for the specification in Equation (1). It reports the elasticity of the effect of upstream deforestation on downstream water and burned-area changes. As we measure all variables in km^2 and open basins have large means, the coefficients can be interpreted as elasticities using the inverse hyperbolic sine transformation.[8]

Water. We find that, on average, a 1% increase in upstream deforestation leads to a 0.51% decrease in water coverage from year to year (Table 2 column 1). This result is based on water coverage data from the Pantanal biome and on the upstream deforestation in the whole hydrographic region.[9]. Adding upstream rainfall in the specification does not affect the result of upstream deforestation, and the coefficient of upstream rainfall is statistically insignificant (Table 2 column 2). This is consistent with the theory that deforestation is the cause of declining water coverage in Pantanal and not changes in upstream rainfall.

It is important to note that the variation we use to estimate the coefficients β and γ is net of year and basin fixed effects. It reflects within-basin year-to-year variation. A potential limitation of relying on this residual variation is that the fixed effects absorb aggregate temporal variation. Indeed, year fixed effects alone have an R^2 of 37% in explaining $\Delta \arcsin(\text{UpRainfall})$—in comparison with a R^2 of 2.5% in explaining $\Delta \arcsin(\text{UpDeforestation})$. While using within-basin year-to-year variation yields no evidence that upstream rainfall affects downstream water coverage, it remains possible that stronger aggregate rainfall variations would have an effect. We also note that it is unlikely that this null effect is the result of hydropower plants in the basin regulating river discharge, because all power plants in the region are run-of-the-river, except one, named Manso.

As discussed before, our identification hypothesis is that changes in upstream deforesta-

[8] See Aïhounton and Henningsen (2019); Bellemare and Wichman (2020) for a detailed discussion on the IHS transformation. These studies argue that when the mean of x is large, the coefficient β can be interpreted as an elasticity. In our analysis, all area-related variables are in km^2 and the non-zero observations (i.e., open basins) have large values of the upstream deforestation, which supports this interpretation. Using the exact elasticity formulas for inverse hyperbolic sine specifications derived by Bellemare and Wichman (2020), and evaluating them at the sample means, yields elasticities that are very close to those implied by the estimated coefficients. The exact elasticity of water coverage is approximately 0.1% more negative, and the exact elasticity of fire is about 0.7% more negative.

[9] Recall from Section 3 that the whole hydrographic region includes the Pantanal biome and surrounding Cerrado highlands, as shown in Figure A1

Table 2: Upstream Deforestation on Water and Fire in the Pantanal

	Water				Fire		
	(1)	(2)	(3)	(4)	(5)	(6)	(7)
Upstream Deforestation	-0.508**	-0.507**			0.554***	0.552***	
	(0.220)	(0.220)			(0.164)	(0.162)	
Upstream Rainfall		0.060				-0.181	
		(0.052)				(0.113)	
Downstream Deforestation			0.040				
			(0.264)				
Future Upstream Deforestation				0.127			-0.172
				(0.100)			(0.177)
Observations	39,976	39,976	39,976	38,924	39,976	39,976	38,924

Notes: This table shows the impact of upstream deforestation on water coverage (columns 1-4) and burned area (columns 5-7) in the Pantanal between 1985 and 2023, as estimated by β in equation 1. All specifications include year fixed effects. All continuous variables (water, fire, and upstream deforestation) are transformed using the inverse hyperbolic sine. Thus, coefficients can be interpreted approximately as elasticities. Column (1) presents the elasticity of water availability to upstream deforestation. Column (2) includes upstream rainfall as a control. Column (3) shows the placebo test with downstream deforestation. Columns (4) and (7) show the placebo test with future upstream deforestation—defined as $\Delta arsin(FutureUpDef_{it)} = arsin(UpDef_{i,t+1}) - arsin(UpDef_{i,t})$. Standard errors (in parentheses) are clustered at level 5 basins (209 clusters). Significance: $p^* < .10$; $p^{**} < .05$; $p^{***} < .01$.

tion are not correlated with other variables that can cause a decrease in downstream water coverage. For example, a productivity shock in one municipality may increase deforestation. If this shock is spatially correlated, it may also induce deforestation downstream. In that case, our results would be biased upward, overstating the impact of upstream deforestation on the outcome of interest.

To further support the claim that omitted variables do not drive our result—specifically that our estimate is not only an effect of spatial correlation—we run a placebo exercise in which we regress downstream deforestation on upstream water coverage, effectively reversing the direction of our basin data. If our estimate were driven solely by spatial correlation, we would expect to find a similar effect in this placebo exercise. Additionally, if the impact on water coverage indeed arises from reduced infiltration and increased sedimentation that disrupt river flows and spring recharge, then downstream deforestation should not affect upstream water coverage, since water cannot travel upstream. Indeed, Table 2 column 3 shows that the estimated impact of downstream deforestation on upstream water coverage is largely insignificant.

As an additional placebo test, we include a lead of deforestation in our first-difference specification. As shown in Table 2 columns (4) and (7), the estimated coefficients on the lead variable are small and statistically insignificant for both outcomes, lending further support to our empirical strategy.

Other possible relevant omitted variables might be human and cattle water consumption and irrigation. Pantanal's population is both small and did not grow fast in the last four decades. In 2021, the biome had close to 380,000 inhabitants, a 25% increase from 1991 compared with an increase of 75% in the total population in Brazil (IBGE, 2021). Irrigation is unlikely to be a relevant mechanism in this context. The total irrigated area in the Pantanal in 2023 amounted to 10,147 hectares, corresponding to only 0.07% of agricultural land and 0.02% of the basin area. Thus, increased irrigation water withdrawals cannot plausibly account for the estimated downstream effects. This is in part because deforestation in the Pantanal is overwhelmingly associated with pasture expansion rather than agriculture. In 2023, 77.2% of deforestation was for pasture formation (86% when areas classified as land-use mosaics are included, representing pasture areas with small-scale agricultural activity), while soybean cultivation accounted for most of the remaining deforested area. As a result, we cannot disentangle whether the estimated effect differs between deforestation associated with pasture versus cropland, or whether it reflects a broader ecological process linked to deforestation more generally. Likewise, increased water consumption by cattle is not large enough to be a meaningful mechanism. Under a highly conservative calculation, cattle consumption of water would account for approximately 0.9% of the biome's available water during the dry season.[10]

Fire. We find that, on average, a 1% increase in the upstream deforestation leads to a 0.55% increase in yearly burned area (Table 2 column 5). This finding is consistent with the mechanism by which reduced water availability leads to drier conditions downstream, increasing the landscape's vulnerability to the spread of wildfires. As in the specification with water coverage as the outcome, adding upstream rainfall to the specification does not affect the result on upstream deforestation, and the rainfall coefficient is only marginally significant, again providing evidence that deforestation is the cause of the observed changes in the Pantanal. Unlike the specification with water coverage as the out-

[10] Assuming that the biome hosts 6.6 million bovine heads in 2022 (IBGE, 2026), and that each animal consumes 38 liters of water per day (Palhares et al., 2021), total annual consumption amounts to approximately 91.6×10^6 m^3. Considering that the biome's flooded area during the dry season covers 4,894 km^2 (MapBiomas Brasil, 2024), with an average water depth of 2 meters (Fantin-Cruz et al., 2011), the total water stock is approximately 9.79×10^9 m^3. Converting cattle consumption to cubic meters and comparing it with the total water volume in the dry season indicates that cattle account for at most 0.9% of the biome's available water.

come, a placebo exercise with downstream deforestation would not be valid, since fire is not constrained by gravity, and the direction of river flow is not the same as that of water.

Indeed, this is a limitation of our analysis, as we do not explicitly model spatial interactions beyond upstream deforestation and downstream water coverage or burned area. There could exist a mechanism that violates the Stable Unit Treatment Value Assumption. For example, if less water is available downstream, it can push cattle ranching upstream. This could be a problem for our identification strategy, biasing our estimated magnitudes upwards, especially if such a mechanism is operating within the same basin and its corresponding upstream basins.

Additional Robustness Checks. As an additional robustness check, we augment our baseline specification with level-3 × year fixed effects, thereby absorbing time-varying shocks common to broader basin groupings. The results, reported in Table A1 columns (1) and (4) in the Appendix, remain qualitatively similar to the baseline, with negative and statistically significant effects on water coverage and burned area.

Millimet and Bellemare (2025) recommends complementing the first-difference estimator with alternative differencing approaches as robustness checks. Accordingly, we implement the rolling first-difference (RFD) estimator described in their paper. The results, reported in Table A1 columns (2) and (5) in the Appendix, are consistent with our baseline findings. While the estimated effect on water coverage is attenuated, it remains negative and statistically significant at the 5% level. The estimated effects on burned area are largely unchanged.

In Table A1, we examine whether upstream deforestation near the observation point has a disproportionate effect on downstream water cover. Columns (3) and (6) show that, conditional on total upstream deforestation, the coefficient on deforestation in the immediately upstream basin is small and statistically insignificant. This pattern is consistent with the geomorphology and hydrology of the Pantanal floodplain (see Assine et al., 2015), in which hydrological influence depends less on geographic proximity and more on the aggregate condition and connectivity of the upstream drainage network.

Finally, Table A2 shows that the results are robust when we allow for basin-specific linear time trends.

A Multiplier Effect on Emissions. We apply our estimates to a back-of-the-envelope calculation to compute the aggregate magnitudes of environmental damage. Between 1985 and 2023, approximately 19,000 km^2 of the Pantanal basin were deforested, representing an 84.6% increase in deforested area. Using our estimated elasticity of water cover-

age reduction with respect to deforestation, we predict a 42.9% decline in water coverage [84.6×0.508], equivalent to approximately 14,323 km^2. This accounts for 53.3% of the total decrease in water coverage observed during the period. A similar calculation can be performed for the burned area. Based on our elasticity estimates, we would expect a 46.87% increase in the burned area [84.6×0.554], corresponding to roughly 9,810 km^2 of burned area. This represents 6% of the total area of the Pantanal biome.

Assuming an average carbon stock of 15,400 metric tons of CO_2 per km^2 in the Pantanal, we estimate that land use conversion alone resulted in approximately 1.029 billion metric tons of CO_2 emissions between 1985 and 2023. Assuming that a burned area releases all of its aboveground carbon stock, based on our elasticity estimate for burned area, the downstream spillover linked to increased fire occurrence accounts for an estimated 151 million metric tons of CO_2. These findings suggest that upstream deforestation not only releases carbon through the direct suppression of natural vegetation but also contributes a non-negligible share of emissions via downstream fire-related impacts. This spillover represents nearly 14% [0.151/1.029] of the total emission attributed directly to deforestation.[11]

6 Conclusions

This paper provides new evidence on how upstream deforestation reduces water coverage and increases area burned in the Pantanal. By exploring a novel panel of satellite-derived data, we show that deforestation contributes to the biome's drying by disrupting hydrological flows.

We also quantify a previously overlooked emissions multiplier associated with deforestation: the loss of vegetation upstream not only releases carbon directly but also weakens the biome's capacity to retain water, thereby increasing the fire occurrence and associated emissions downstream. This mechanism strengthens the case for integrating hydrological spillovers into deforestation policy assessments, which often consider emissions in isolation. Recognizing this feedback is especially important in biomes like the Pantanal, where water flows connect protected and unprotected areas across national and subnational boundaries.

[11] This considers the average of 153.9 tCO_2 per hectare for the Pantanal, as reported by MCTI (2022). It is important to note that this represents a lower-bound estimate, as it considers the lower carbon concentration in the Pantanal region. As the Cerrado has, on average, more carbon per hectare (178.8 tCO_2/ha), actual fire-related emission releases more carbon dioxide there.

Beyond basin-mediated channels, broader atmospheric spillovers remain plausible: in particular, deforestation in other regions—most notably the Amazon—may influence Pantanal hydrology through rainfall recycling and regional climate feedbacks (Salati et al., 1979; Araujo, 2023). Our empirical design isolates hydrological transmission within basins and therefore does not capture these wider climatic mechanisms.

Our results contribute to a growing body of research that emphasizes the importance of ecological interdependence in environmental policy design. In the case of the Pantanal, failing to account for hydrological spillovers can lead to misinformed land use decisions and regulatory inefficiencies. Future work could explore how institutional arrangements, such as protected area design, water governance, or land market regulation, can be adapted to internalize these spatial spillovers.

References

ANA (2006). *Codificação de Bacias Hidrográficas pelo Método de Otto Pfafstetter: Aplicação na ANA*. Agência Nacional de Águas.

ANA (2020). Base hidrográfica ottocodificada (bho). https://metadados.snirh.gov.br/geonetwork/srv/api/records/b228d007-6d68-46e5-b30d-a1e191b2b21f. Accessed: 2023-10-05.

Anderson, T. W. and Hsiao, C. (1981). Estimation of dynamic models with error components. *Journal of the American Statistical Association*, 76(375):598–606.

Araujo, R. (2023). When clouds go dry: An integrated model of deforestation, rainfall, and agriculture. *Job Market Paper*.

Araujo, R., Costa, F., and Sant'Anna, M. (2026). Efficient Conservation of the Brazilian Amazon: Estimates from a Dynamic Model. *Review of Economic Studies*, 93(1):72–105.

Arellano, M. and Bond, S. (1991). Some tests of specification for panel data: Monte carlo evidence and an application to employment equations. *Review of Economic Studies*, 58(2):277–297.

Aronoff, D. and Rafey, W. (2023). Conservation Priorities and Environmental Offsets: Markets for Florida Wetlands. Technical Report w31495, NBER, Cambridge, MA.

Assine, M. L., Macedo, H. A., Stevaux, J. C., Bergier, I., Padovani, C. R., and Silva, A. (2015). Avulsive rivers in the hydrology of the pantanal wetland. In *Dynamics of the Pantanal Wetland in South America*, pages 83–110. Springer.

Assunção, J., Gandour, C., and Rocha, R. (2013). Deterring deforestation in the brazilian amazon: environmental monitoring and law enforcement. *Climate Policy Initiative*, 1:36.

Assunção, J., Gandour, C., Rocha, R., and Rocha, R. (2020). The effect of rural credit on deforestation: evidence from the brazilian amazon. *Economic Journal*, 130(626):290–330.

Aïhounton, G. B. D. and Henningsen, A. (2019). Units of measurement and the inverse hyperbolic sine transformation. *IFRO Working Paper*, 1(2019/10).

Bellemare, M. F. and Wichman, C. J. (2020). Elasticities and the Inverse Hyperbolic Sine Transformation. *Oxford Bulletin of Economics and Statistics*, 82(1):50–61.

Bergier, I. (2013). Effects of highland land-use over lowlands of the Brazilian Pantanal. *Science of The Total Environment*, 463-464:1060–1066.

Bergier, I. and Assine, M. L. (2022). Functional fluvial landforms of the Pantanal: Hydrologic trends and responses to climate changes. *Journal of South American Earth Sciences*, 119:103977.

Bergier, I., Assine, M. L., McGlue, M. M., Alho, C. J., Silva, A., Guerreiro, R. L., and Carvalho, J. C. (2018). Amazon rainforest modulation of water security in the Pantanal wetland. *Science of The Total Environment*, 619-620:1116–1125.

Brody, S. D., Highfield, W. E., and Blessing, R. (2015). An analysis of the effects of land use and land cover on flood losses along the gulf of mexico coast from 1999 to 2009. *JAWRA Journal of the American Water Resources Association*, 51(6):1556–1567.

Burgess, R., Costa, F., and Olken, B. A. (2023). National Borders and the Conservation of Nature. *OSF, Available at OSF: https://osf. io/preprints/socarxiv/67xg5*.

Chen, Z., Kahn, M. E., Liu, Y., and Wang, Z. (2018). The consequences of spatially differentiated water pollution regulation in China. *Journal of Environmental Economics and Management*, 88:468–485.

Climate Hazards Center (2023). Climate hazards group infrared precipitation with station data (chirps). https://www.chc.ucsb.edu/data/chirps. Version 3.0. Accessed: 2025-02-06.

Dias, M., Rocha, R., and Soares, R. R. (2023). Down the River: Glyphosate Use in Agriculture and Birth Outcomes of Surrounding Populations. *Review of Economic Studies*, 90(6):2943–2981.

Domínguez-Iino, T. (2026). Efficiency and redistribution in environmental policy: An equilibrium analysis of agricultural supply chains. *Journal of Political Economy*.

Ebenstein, A. (2012). The Consequences of Industrialization: Evidence from Water Pollution and Digestive Cancers in China. *Review of Economics and Statistics*, 94(1):186–201.

Fantin-Cruz, I., Pedrollo, O., Castro, N. M., Girard, P., Zeilhofer, P., and Hamilton, S. K. (2011). Historical reconstruction of floodplain inundation in the pantanal (brazil) using neural networks. *Journal of Hydrology*, 399(3):376–384.

Giglio, L., Justice, C., Boschetti, L., and Roy, D. (2015). MCD64A1 MODIS/Terra+Aqua Burned Area Monthly L3 Global 500m SIN Grid, Version 6. Accessed: July 2025, 2026. https://www.earthdata.nasa.gov/data/catalog/lpcloud-mcd64a1-006.

Global Commission on the Economics of Water (2024). The Economics of Water: Valuing the Hydrological Cycle as a Global Common Good. Technical report, Global Commission on the Economics of Water.

Hagerty, N. (2023). What holds back water markets? transaction costs and the gains from trade. *Working Paper*.

IBGE (2021). *Estimativas da população : 2021*. Coleção Ibgeana. Instituto Brasileiro de Geografia e Estatística (IBGE), [Rio de Janeiro].

IBGE (2026). Pesquisa da pecuária municipal (ppm), tabela 3939: Efetivo dos rebanhos, por tipo de rebanho. Sistema IBGE de Recuperação Automática (SIDRA). Accessed: February 16, 2026. https://sidra.ibge.gov.br/tabela/3939.

Instituto Nacional de Pesquisas Espaciais (INPE) (2023). Banco de dados de queimadas (bdqueimadas). http://www.inpe.br/queimadas/bdqueimadas. Accessed: 2025-02-06.

Ivory, S. J., McGlue, M. M., Spera, S., Silva, A., and Bergier, I. (2019). Vegetation, rainfall, and pulsing hydrology in the Pantanal, the world's largest tropical wetland. *Environmental Research Letters*, 14(12):124017.

Karwowski, N. (2024). Estimating the effect of easements on agricultural production. In *American Agriculture, Water Resources, and Climate Change*, pages 53–106. University of Chicago Press.

Leal Filho, W., Azeiteiro, U. M., Salvia, A. L., Fritzen, B., and Libonati, R. (2021). Fire in Paradise: Why the Pantanal is burning. *Environmental Science & Policy*, 123:31–34.

Libonati, R., DaCamara, C. C., Peres, L. F., Sander De Carvalho, L. A., and Garcia, L. C. (2020). Rescue Brazil's burning Pantanal wetlands. *Nature*, 588(7837):217–219.

Lipscomb, M. and Mobarak, A. M. (2017). Decentralization and Pollution Spillovers: Evidence from the Re-drawing of County Borders in Brazil. *Review of Economic Studies*, 84(1):464–502.

Long, T., Zhang, Z., He, G., Jiao, W., Tang, C., Wu, B., Zhang, X., Wang, G., and Yin, R. (2019). 30 m Resolution Global Annual Burned Area Mapping Based on Landsat Images and Google Earth Engine. *Remote Sensing*, 11(5):489.

Lázaro, W. L., Oliveira-Júnior, E. S., Silva, C. J. D., Castrillon, S. K. I., and Muniz, C. C. (2020). Climate change reflected in one of the largest wetlands in the world: an overview of the Northern Pantanal water regime. *Acta Limnol. Bras.*, 32:e104.

MapBiomas Brasil (2024). Collection 9 of the Annual Series of Land Cover and Use Maps of Brazil. https://mapbiomas.org. Accessed on January 22, 2025.

MapBiomas Brasil (2025a). Download dos atbds com método detalhado. Accessed on January 22, 2025.

MapBiomas Brasil (2025b). Legenda coleção 9 - legend code v2. Accessed on January 22, 2025.

Marengo, J. A., Cunha, A. P., Cuartas, L. A., Deusdará Leal, K. R., Broedel, E., Seluchi, M. E., Michelin, C. M., De Praga Baião, C. F., Chuchón Angulo, E., Almeida, E. K., Kazmierczak, M. L., Mateus, N. P. A., Silva, R. C., and Bender, F. (2021). Extreme Drought in the Brazilian Pantanal in 2019–2020: Characterization, Causes, and Impacts. *Front. Water*, 3:639204.

MCTI (2022). *Quarta comunicação nacional do Brasil à Convenção Quadro das Nações Unidas sobre Mudança do Clima*. Ministério da Ciência, Tecnologia e Inovações, Brasília, DF.

Millimet, D. L. and Bellemare, M. F. (2025). On the (mis) use of the fixed effects estimator. *Oxford Bulletin of Economics and Statistics*.

NASA JPL (2013). NASA Shuttle Radar Topography Mission Global 1 arc second. Accessed: July 2025. https://www.earthdata.nasa.gov/data/catalog/lpcloud-srtmgl1-003#toc-description.

Palhares, J. C. P., Morelli, M., and Novelli, T. I. (2021). Water footprint of a tropical beef cattle production system: The impact of individual-animal and feed management. *Advances in Water Resources*, 149:103853.

Paz, A. R. D., Collischonn, W., Tucci, C. E. M., and Padovani, C. R. (2011). Large-scale modelling of channel flow and floodplain inundation dynamics and its application to the Pantanal (Brazil). *Hydrological Processes*, 25(9):1498–1516.

Peña-Arancibia, J. L., Bruijnzeel, L. A., Mulligan, M., and Van Dijk, A. I. (2019). Forests as 'sponges' and 'pumps': Assessing the impact of deforestation on dry-season flows across the tropics. *Journal of Hydrology*, 574:946–963.

Rafey, W. (2023). Droughts, deluges, and (river) diversions: Valuing market-based water reallocation. *American Economic Review*, 113(2):430–471.

Rohde, M. M., Stella, J. C., Roberts, D. A., and Singer, M. B. (2021). Groundwater dependence of riparian woodlands and the disrupting effect of anthropogenically altered streamflow. *Proceedings of the National Academy of Sciences*, 118(25):e2026453118.

Rosa, E., Ribeiro, J. P., Shimbo, J., Martenexen, L. F., Dias, M., Monteiro, N. C., Arruda, V. L. d. S., and Silva, W. V. d. (2025). Nota Técnica: Seca extrema e incêndios no Pantanal em 2024. Technical note, MapBiomas. Accessed: July 2025.

Salati, E., Dall'Olio, A., Matsui, E., and Gat, J. R. (1979). Recycling of water in the amazon basin: An isotopic study. *Water Resources Research*, 15(5):1250–1258.

Sant'Anna, M. (2021). How Green Is Sugarcane Ethanol? *The Review of Economics and Statistics*, pages 1–45.

Santos, F. C., Chaves, F. M., Negri, R. G., and Massi, K. G. (2024). Fires in Pantanal: The link to Agriculture, Conversions in Cerrado, and Hydrological Changes. *Wetlands*, 44(6):75.

Skidmore, M. E., Sims, K. M., and Gibbs, H. K. (2023). Agricultural intensification and childhood cancer in brazil. *Proceedings of the National Academy of Sciences*, 120(45):e2306003120.

Souza-Rodrigues, E. (2019). Deforestation in the amazon: A unified framework for estimation and policy analysis. *Review of Economic Studies*, 86(6):2713–2744.

Sun, F. and Carson, R. T. (2020). Coastal wetlands reduce property damage during tropical cyclones. *Proceedings of the National Academy of Sciences*, 117(11):5719–5725.

Taylor, C. A. and Druckenmiller, H. (2022). Wetlands, flooding, and the clean water act. *American Economic Review*, 112(4):1334–1363.

Weitzman, M. L. (1974). Prices vs. quantities12. *Review of Economic Studies*, 41(4):477–491.

WWF (2018). Conserving the World's Largest Wetland: The Pantanal. Factsheet, World Wildlife Fund (WWF). Accessed: January 2025.

Yu, G., Xiu, C., Zhao, C., and Ding, Z. (2018). Strategic Cross-Border Water Pollution in Songliao Basin. *Sustainability*, 10(12):4713.

A Appendix

A1 Pantanal's Geography

The Pantanal results from the interaction of topography and hydrology. Rainfall falls on the surrounding Cerrado highlands and flows downstream. Because the biome is a vast plain, water accumulates and forms thousands of lagoons that sustain its ecosystem. Figure A1 shows this dynamic spatially.

Figure A1: Pantanal's Topography and Hydrology

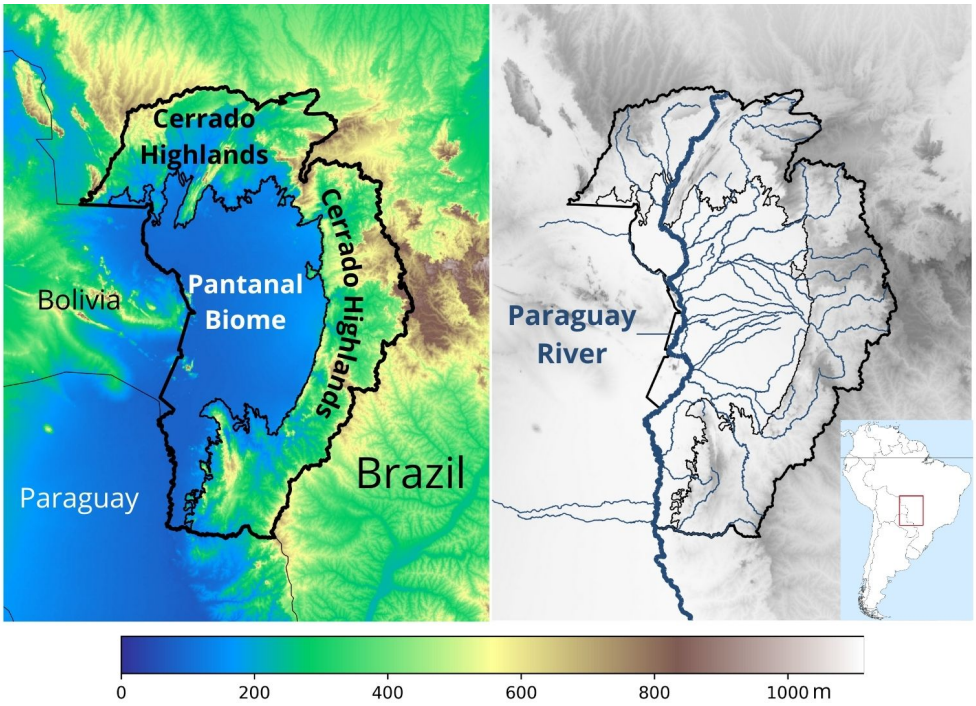

Notes: This figure shows the region's topography (left) and hydrology (right). It highlights the plain relief of the biome and the role of the Cerrado highlands in the water balance.
Sources: NASA JPL (2013); ANA (2020)

This paper studies how land use change in the whole Pantanal basin (biome plain + the Cerrado highlands) affects outcomes in the Pantanal biome. The region's rivers are the channels through which these effects flow.

A2 Pfafstetter Method

We use the Pfafstetter Method (also known as Ottocodification) to map each basin with its upstream area (ANA, 2006). Figure A2 (A) illustrates the method.

The steps are as follows. First, define a hydrographic basin as the land where all water flows to a single pour point. The idea is that if water is poured anywhere in the basin, it will end up at that point. Next, map the basin's main river and the four tributaries with the largest catchment areas. Then map the five remaining intermediate areas. Finally, assign codes: use the same radical and add digits 1 to 9, moving from downstream to upstream. Even numbers mark tributary basins, while odd numbers mark interbasins.

Figure A2: Illustration of the Pfafstetter Coding System

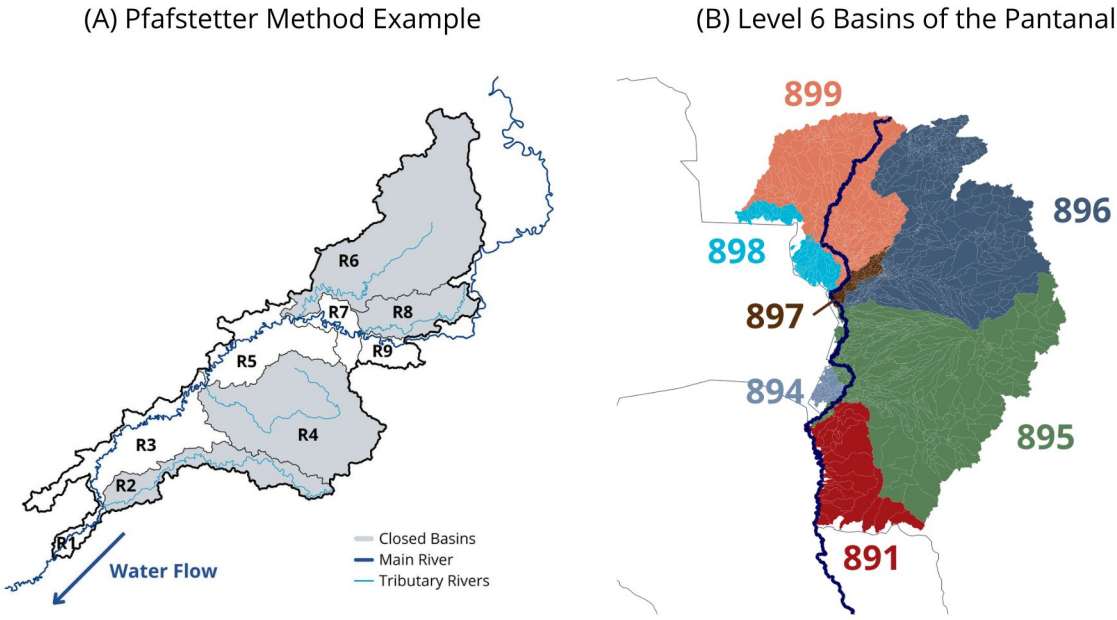

Notes: (A) shows the Pfafstetter Coding System using the level 6 basins within level 5 basin $R = 89651$. R stands for radical. The level 6 basins are numbered sequentially from downstream to upstream, 896511 to 896519. Closed basins are even-numbered (R2, R4, R6, R8) and have no upstream inflows. Open basins are odd-numbered (R1, R3, R5, R7, R9) and receive water from other basins, including those outside the level 5 basin. See ANA (2006) for details. (B) shows all 1,873 level 6 basins used to build the panel. The three-digit Pfafstetter codes (891 to 899) mark the level 3 basins that group each set of level 6 basins. All water in the region drains into the Paraguay River, shown in blue.
Source: ANA (2020, 2006)

There are seven levels of hydrographic basins, with level 1 the least detailed, such as the Amazon and Paraná ones. We use level 6 basins as they are detailed enough to identify effects while still feasible for panel construction.

ANA (2020) provides Pfafstetter codes for every basin in the South America. We apply the algorithm to all 1,873 level 6 basins in the Pantanal hydrographic region to identify their upstream areas. We then merge this with land use and land cover (LULC) data from

MapBiomas Brasil (2024). For each basin and year between 1985 and 2023, we compute the upstream area under deforestation. Figure A3 (B) shows a map of all basins we consider to build the panel.

Figure A3: LULC Example

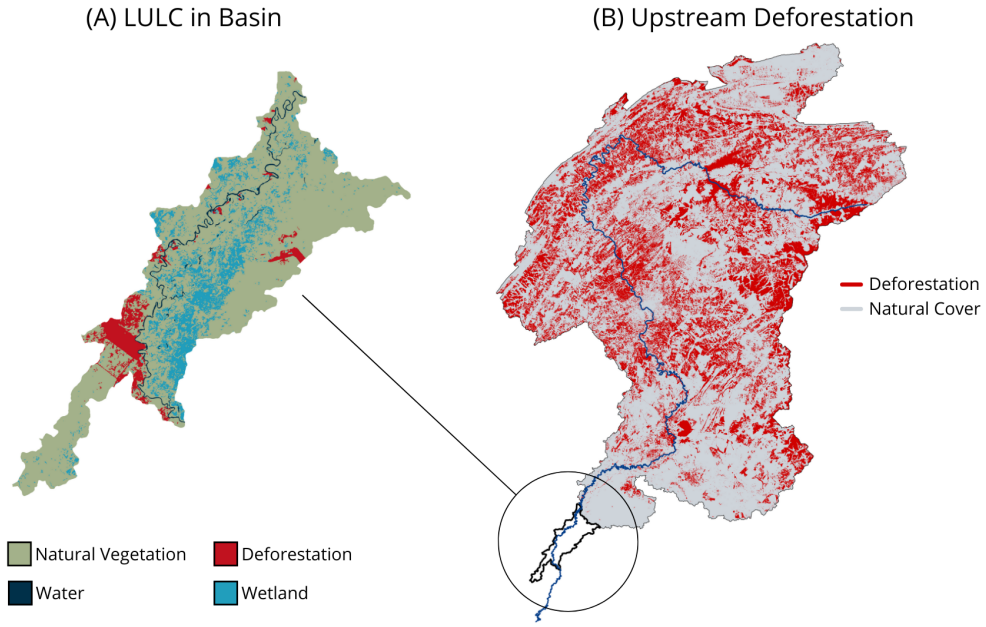

Notes: Example for basin 896513 and its upstream area. Upstream deforestation includes pasture, agriculture, mining, and cities. This is an open basin. Closed basins have no upstream area and thus zero upstream deforestation. Panel (B) highlights in blue the main river that carries upstream water downstream. Smaller tributaries are omitted.

A3 Additional Tables

We perform a series of additional exercises to assess the robustness of our findings presented in Section 5. Table A1 reports the results.

Columns (1) and (4) reproduce the baseline specification in Equation 1, replacing the original fixed effects with Level 3 $\times$ year fixed effects for water and fire outcomes, respectively. These fixed effects absorb time-varying shocks common to broader basin groupings. The estimated coefficients remain statistically significant and retain the same sign as in the baseline specification.

Columns (2) and (5) present estimates of the main specification obtained using a rolling first-difference (RFD) estimator, following Millimet and Bellemare (2025). The results are again statistically significant and consistent in direction with the main specification at Equation (1).

Finally, columns (3) and (6) expand the model by controlling for upstream deforestation in the basin immediately upstream. This allows us to assess whether the effects operate through nearby deforestation. The point estimates have the same sign but are substantially smaller and are statistically indistinguishable from zero. This suggests that the observed impacts on water and fire outcomes are not driven only by deforestation directly upstream, but rather reflect broader spatial dynamics.

Table A1: Additional Robustness Checks

	Water			Fire		
	(1)	(2)	(3)	(4)	(5)	(6)
Upstream Deforestation	-0.256**	-0.314***	-0.479**	0.301***	0.546***	0.520**
	(0.121)	(0.029)	(0.236)	(0.105)	(0.047)	(0.162)
Direct Up. Deforestation			-0.065			0.075
			(0.068)			(0.062)
Estimator	FD	RFD	FD	FD	RFD	FD
Year FE	No	Yes	Yes	No	Yes	Yes
Level 3 x Year FE	Yes	No	No	Yes	No	No
Observations	39,976	41,028	39,976	39,976	41,028	39,976

Notes: This table shows additional robustness checks to the main specification at Table 2. Columns (1-3) show results for water coverage, and columns (4-6) show results for burned area as the outcome. Columns (1) and (4) present the point estimates considering Level 3 basin $\times$ year fixed effects, instead of only year fixed effects. Columns (2) and (5) estimate the baseline specification using the Rolling First Difference estimator (RFD) from Millimet and Bellemare (2025). Columns (3) and (6) estimate the baseline specification from equation (1) and include the first difference of deforestation in the basin's immediate upstream basin, that is, the first direct upstream basin. Standard errors (in parentheses) are clustered at level 5 basins (209 clusters). Significance: $p^{*} < .10$; $p^{**} < .05$; $p^{***} < .01$.

We also test an alternative specification with basin-specific linear time trends. The purpose of this specification is to investigate the impact of basin-specific dynamics on water and fire outcomes. Table A2 shows the results. Columns (1) and (2) show that the magnitude and sign of the effects, accounting for basin-trends, are similar to the main specification at Equation 1 for water. Columns (3) and (4) show the same for fire. This suggests that basin trends do not change the magnitude of the effects of upstream deforestation, thus strengthening our results.

Table A2: Alternative Specification with Basin-specific Time Trend

	Water		Fire	
	(1)	(2)	(3)	(4)
Upstream Deforestation	-0.560**	-0.559**	0.648***	0.646***
	(0.250)	(0.249)	(0.189)	(0.187)
Upstream Rainfall		0.062		-0.180
		(0.052)		(0.113)
Basin FE	Yes	Yes	Yes	Yes
Observations	39,976	39,976	39,976	39,976

Notes: This table shows an alternative specification to the main results in Table 2, including basin-specific trends—i.e., we include Level 5 basisn fixed effects in equation (1). All specifications include year fixed effects. Columns (1-2) show results for water coverage, and columns (3-4) show results for burned area as the outcome. Standard errors (in parentheses) are clustered at level 5 basins (209 clusters). Significance: $p^{*} < .10$; $p^{**} < .05$; $p^{***} < .01$.